Sensors & Actuators: A. Physical 377 (2024) 115713

Contents lists available at ScienceDirect

Sensors and Actuators: A. Physical

journal homepage: www.journals.elsevier.com/sensors-and-actuators-a-physical

# Investigation of the free-base Zr-porphyrin MOFs as relative humidity sensors for an indoor setting

Nicholaus Prasetya *, Salih Okur

*Institute of Functional Interface (IFG), Karlsruhe Institute of Technology, Hermann-von-Helmholtz-Platz 1, Eggenstein-Leopoldshafen 76344, Germany*

ARTICLE INFO

*Keywords:*
Relative humidity
QCM sensors
Zr-porphyrin metal-organic framework
Adsorption

ABSTRACT

Maintaining optimal relative humidity is paramount for human comfort. Therefore, the utilization of quartz crystal microbalance (QCM) as a relative humidity sensor platform holds significant promise due to its cost-effectiveness and high sensitivity. This study explores the efficacy of three free-base Zr porphyrin metal-organic frameworks (MOFs) - namely MOF-525, MOF-545, and NU-902 - as sensitive materials for QCM-based relative humidity sensors. Our extended experimental findings reveal that these materials exhibit notable sensitivity, particularly within relative humidity ranges of 40–100 %. However, we observe potential irreversible adsorption sites within the MOF-545 framework, hindering its ability to revert to its initial state after prolonged exposure. In light of this observation, we conduct periodic cycling experiments at relative humidity levels of 40–70 % to evaluate the measurement repeatability and feasibility of these sensors for indoor applications. Interestingly, the periodic cycling study demonstrates that MOF-545 shows promising repeatability, positioning it as a strong contender for indoor relative humidity sensing. In contrast, MOF-525 may necessitate extended desorption time, and NU-902 displays diminished sensitivity at low relative humidity levels. Nevertheless, a preliminary treatment of the MOF-545 QCM sensor may be necessary to address irreversible adsorption sites and uphold measurement repeatability, as only reversible adsorption sites are currently accessible. This study underscores the potential of MOF-based QCM sensors for effective relative humidity monitoring in indoor environments, thus facilitating improved comfort and environmental control.

## 1. Introduction

Relative humidity control plays a vital role in various settings including to maintain the comfort of human beings in an indoor setting where the relative humidity level is expected to be maintained around 40–70 % [1,2]. The importance lies in the fact that maintaining the indoor relative humidity is crucial to preserve the healthy environment for human beings. When the relative humidity is too low, various health issues such as skin dryness and rash, pharyngeal dryness and nasal dryness could occur [3]. Meanwhile, when the relative humidity level is too high, it could accelerate the microbial growth and increase the risk of house dust mite infestation [4]. Therefore, the use of a reliable, highly sensitive and cheap relative humidity sensor becomes inevitable. To achieve this objective, there is a growing interest in the research and development of such sensors that can fulfill these criteria. Therefore, there are different type of relative humidity sensors, which could be based on the generation of electrical or optical signals [5–8]. In comparison to these sensors, a relative humidity sensor fabricated based on the quartz crystal microbalance (QCM) platform has several advantages since it is highly sensitive, can usually be produced at low cost and can also offer handling convenience thanks to its small size. To date, various materials have been investigated for this purpose such as graphene-based materials [9,10], $SnO_2$ nanowires [11], ruthenium polypyridyl complex [12], polymethylmethacrylate micropillar [13] and various composites that can combine the properties of different materials, such as polyaniline/graphene oxide [14], graphene oxide/poly(ethyleneimine) [15], graphene quantum dots/chitosan [16], fullerene/graphene oxide [17] and polyvinylalcohol/ZnO [18].

Metal-organic framework (MOF) is a porous material constructed by metal clusters linked by organic ligands. In comparison to other porous materials, MOF offers a number of advantages such as high surface area, high porosity, and tailorable architecture. Research and development of MOF has been ongoing for more than two decades and still attracts high interest since it can be used for various purposes such as a platform for a new material [19,20], gas separation process [21,22], as adsorbents to remove of various pollutants from the water streams [23,24] and as a

* Corresponding author.
*E-mail address:* nicholaus.prasetya@partner.kit.edu (N. Prasetya).

https://doi.org/10.1016/j.sna.2024.115713
Received 8 May 2024; Received in revised form 11 July 2024; Accepted 14 July 2024
Available online 15 July 2024

sensitive layer in a sensor [25–27]. In this study, we investigate the use of three free-base porphyrin MOFs as a relative humidity sensor material, namely MOF-525, MOF-545 and NU-902. As has been previously reported, these MOFs can be synthesized from the same building block by adjusting the reaction conditions and modulator [28]. These MOFs are particularly chosen because they have large surface areas and pore apertures that can accommodate water molecules and possess robust framework that is resistant to water rendering them suitable for various water-based applications [28–31]. In fact, the feasibility of these MOFs for various sensor applications have been investigated. For example, MOF-525 has been investigated to be used as part of a composite biosensor in tandem with poly(3,4-ethylenedioxythiophene) nanotube (PEDOT NTs) as a dopamine sensor [32]. While the MOF-525 acts as the electrocatalytic surface, the PEDOT NTs has a role as a charge collector to transport the electron from the MOF-525. Another high-sensitivity biosensor with relatively low limit of detection to be around 0.13 μg $mL^{-1}$ has also been studied using MOF-545 which is constructed as a photoelectrochemical sensor to detect phosphoprotein (α-casein) [33]. Meanwhile, NU-902 has also shown its efficacy as a nitrite sensor when its pore is loaded with silver nanoparticle since they both have a role as an electrocatalyst for nitrite oxidation [34]. Moreover, in addition to the electrocatalyst-based sensors as mentioned in the above examples, these free-base porphyrin MOFs can also be used as colorimetric sensors. This potential has then been exemplified in the case of both MOF-525 and MOF-545/PCN-222 which have been previously studied as colorimetric-based sensor that are responsive against change in pH [35–37]. All these investigations have then shown the promising sensor applications of the selected porphyrin MOFs used in this study. Therefore, this study aims to further expands the horizon of the sensor applicability of the free-base porphyrin MOFs, particularly as a humidity sensor which can be constructed based on the use of QCM and thus, as has been discussed above, offering the possibility to construct highly-reliable MOF-based humidity sensor at a low cost.

## 2. Materials and methods

### 2.1. Materials

Benzoic acid (99 %), 4-methoxybenzoic acid (≥ 98.0 %) and zirconyl chloride octahydrate ($ZrOCl_2.8\,H_2O$, 98 %) were purchased from Merck. Meso-tetra(4-carboxyphenyl)porphyrin ($H_4TCPP$, 97 %) was purchased from BLD Pharmatech GmbH, Germany. Acetone (99.5 %), dimethylformamide (DMF, 99.5 %), formic acid 99 %, hydrochloric acid 37 % was purchased from VWR. SiOx-coated gold 5 MHz QCM sensors were purchased from Novaetech S.r.l, Italy. The relative humidity and temperature sensor were purchased from Sensirion (SHT4xA).

### 2.2. MOF synthesis

All the Zr free-base porphyrin MOFs used in this study, namely MOF-525, MOF-545 and NU-902, are illustrated in the Fig. 1 and they were synthesized according to the previous study by using the identical metal and ligand source but different modulator [28]. The powder X-ray diffraction (PXRD) patterns, Fourier-transformed infrared (FTIR) spectra and the micrographs of the samples were collected by using a D8 A25 Da-Vinci Bruker XRD, Bruker Hyperion - Tensor in Attenuated Total Reflectance (ATR) mode and scanning electron microscope (SEM) XL30, respectively.

### 2.3. QCM sensor preparation

In this experiment, SiOx-coated gold QCM were used. Prior to use, all the QCM sensors were thoroughly cleaned with ethanol and then treated with UV light for approximately 7 minutes to clean the surface. Subsequently, a MOF suspension in ethanol (1 mg $mL^{-1}$) was carefully drop-cast on the QCM surface using a small plastic pipette. Throughout the drop-casting process, the QCM frequency was continuously monitored to observe the mass change which was reflected as a change in the QCM frequency. The drop-casting process was repeated several times until the required mass was obtained.

### 2.4. Relative humidity sensing

The relative humidity sensing experiment was conducted following the previous method and illustrated in Fig. 2 [12]. As can be seen, in this experiment, the relative humidity was controlled by using aqueous solutions saturated with different salts [38]. Therefore, initially, several aqueous solutions saturated with different salts were prepared in an enclosed vial to generate environments with varying value of relative humidity. Subsequently, one bare QCM sensor, along with three QCM sensors coated with MOF-525, MOF-545 and NU-902 as the sensitive material, were carefully hanged just above the saturated salt solution, along with the relative humidity sensor (Sensirion SHT4xA). This was done because, even though the relative humidity in the vial is determined by the vapor pressure of the saturated salt solutions, its value might still be slightly affected by other parameters such as the salt and

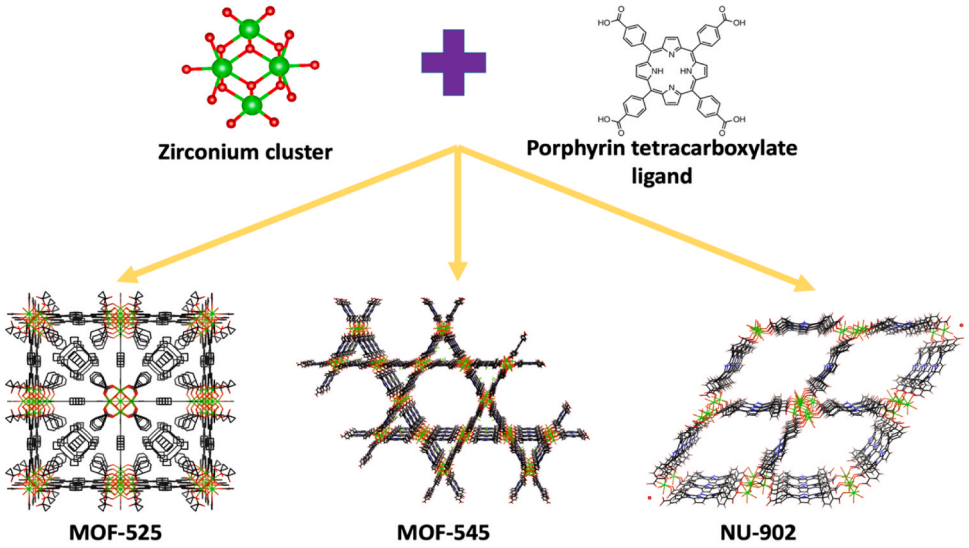


**Fig. 1.** Illustration of the building blocks and the view of MOF-525, MOF-545 and NU-902.

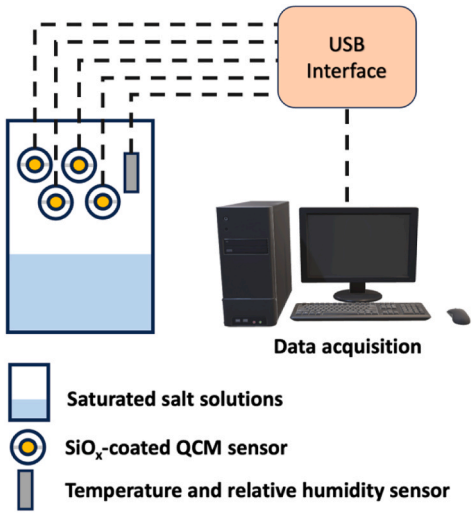


| Relative humidity (%) | Saturated salt solution |
|---|---|
| 6 | Pottasium hydroxide |
| 18.6 | Potassium acetate |
| 36.12 | Magnesium chloride |
| 45.5 | Potassium carbonate |
| 70 | Potassium iodide |
| 74.7 | Sodium chloride |
| 79.5 | Potassium chloride |
| 90.3 | Potassium nitrate |
| 97 | Water |

**Fig. 2.** An illustration of the experimental setup used to measure the water vapor uptake of free-base Zr-porphyrin MOF QCM sensors at different relative humidity.

water purity, a slight change in the surrounding temperature and also a slight exposure to the surrounding environment. Therefore, a relative humidity sensor reading is necessary to always record the actual value. The readings were taken until the equilibrium was reached, indicated by no further change in the QCM frequency. The process was conducted sequentially, from the lowest relative humidity to the highest during the adsorption process and vice versa during the desorption process. Throughout the investigation, QCM frequencies were recorded in all conditions: namely before ($f_0$) and after ($f_1$) drop-casting with MOF suspension and during exposure at different relative humidity levels ($f_2$). It should also be noted that the $f_2$ value must also be corrected against the QCM blank sample since the SiOx-coated gold QCM also shows a small amount of water vapor adsorption, as indicated by the change of the QCM frequency, as shown in the Figure S1 in the Supplementary Information. All the experiments were conducted at room temperature ($\pm$ $25^0$ C).

## 3. Results and discussions

In this study, we selected three isomers of Zr free-base porphyrin MOFs, namely MOF-525, MOF-545 and NU-902, as the sensor material for relative humidity sensing. Although all the MOFs are constructed using the same building block, as illustrated in the Fig. 1, they exhibit topological difference. The topology of MOF-525, MOF-545 and NU-902 is **ftw**, **csq** and **scu**, respectively. Despite this topological difference, from our previous observation by using argon physisorption and employing the non-localized density functional theory (NLDFT) model, we found that the surface area of MOF-525, MOF-545 and NU-902 is quite similar to each other, namely just below 2000 $m^2\,g^{-1}$ with the pore size distribution peaking in the range of 1.5 – 2 nm [28]. Therefore, considering their robust framework under humid conditions and their large pore size and surface area [28], we hypothesize that these MOFs might also become excellent candidates as sensor materials for relative humidity sensing since they might also exhibit good adsorption capability towards water vapor.

This hypothesis is based on the previous study involving three different types of MOFs for water vapor adsorption, namely MOF with small pores (e.g., UiO-66 and MOF-801), large pores (e.g., MOF-808 and DUT-67) and with hydroxyl-functional group (e.g., MOF-804, MOF-805 and MOF-806) [39]. From the investigation, it is revealed that, in general, MOFs with large pore diameter between 0.8 – 1.84 nm have exhibited the highest total water vapor uptake compared with the MOFs with small pores or with hydroxyl functional group. Moreover, when such large-pore MOFs are relatively hydrophobic, their water vapor uptake at low partial pressure is very limited and the uptake usually stats at $P/P_0$ around 0.2–0.3. In the context of employing MOF as a relative humidity sensor material in an indoor setting, where the relative humidity must be maintained in the range of 40–70 %, this brings an advantage since the MOFs might not have yet reached their equilibrium uptake within this relative humidity range and thus could still be very sensitive as a sensor material. This is in contrast with small-pore MOFs or MOFs with hydroxyl functional groups where the water vapor uptake begins at low partial pressure and, therefore, might have reached the saturation point at $P/P_0$ below 0.4. As a consequence, such MOFs might not be sensitive anymore in the relative humidity range of 40–70 % and therefore not suitable to be used as a relative humidity sensor material in an indoor setting. In the case of our free-base porphyrin MOFs without any hydrophilic functional groups, it could then be considered that the framework itself is relatively hydrophobic [40]. Therefore, along with their large pore size and surface area, it could also be expected that their water vapor uptake at low partial pressure is also relatively low and, as a result, they could still be very sensitive in the relative humidity range between 40 % and 70 % since their water vapor uptake saturation point has not yet been reached.

### 3.1. *Relative humidity sensing of MOF-525, MOF-545 and NU-902 during extended experiment time*

Before conducting the extended experiment time investigation, the MOFs used in this study were firstly characterized by obtaining their PXRD patterns, FTIR spectra and micrographs as given in the Fig. 3. As can be seen in the result, all the MOFs used in this study were highly crystalline and they exhibit identical FTIR spectra since they are constructed using the same starting material. From the micrographs, it can also be seen that both MOF-525 and NU-902 crystalizes into a spherical shape while MOF-545 crystallizes into a rod shape.

Afterwards, all the MOFs were used in the extended experiment time investigation where the water vapor adsorption-desorption for all the MOF QCM sensors exposed to different relative humidity levels were carried out at relatively long period of time to ensure the equilibrium has been reached. The result for this investigation is then presented in the Fig. 4(A). From the results, it can be observed that all the MOF QCM samples exhibit a negative QCM frequency trend. This contrasts with the previous work showing the possibility of having a positive QCM frequency shift when using MOF as a sensitive layer in a QCM sensor [41]. This trend might then be attributed to the use of SiOx-coated gold QCM sensors, which could enhance the interaction between the MOF and the QCM surface. Such a strong interaction might contribute in a

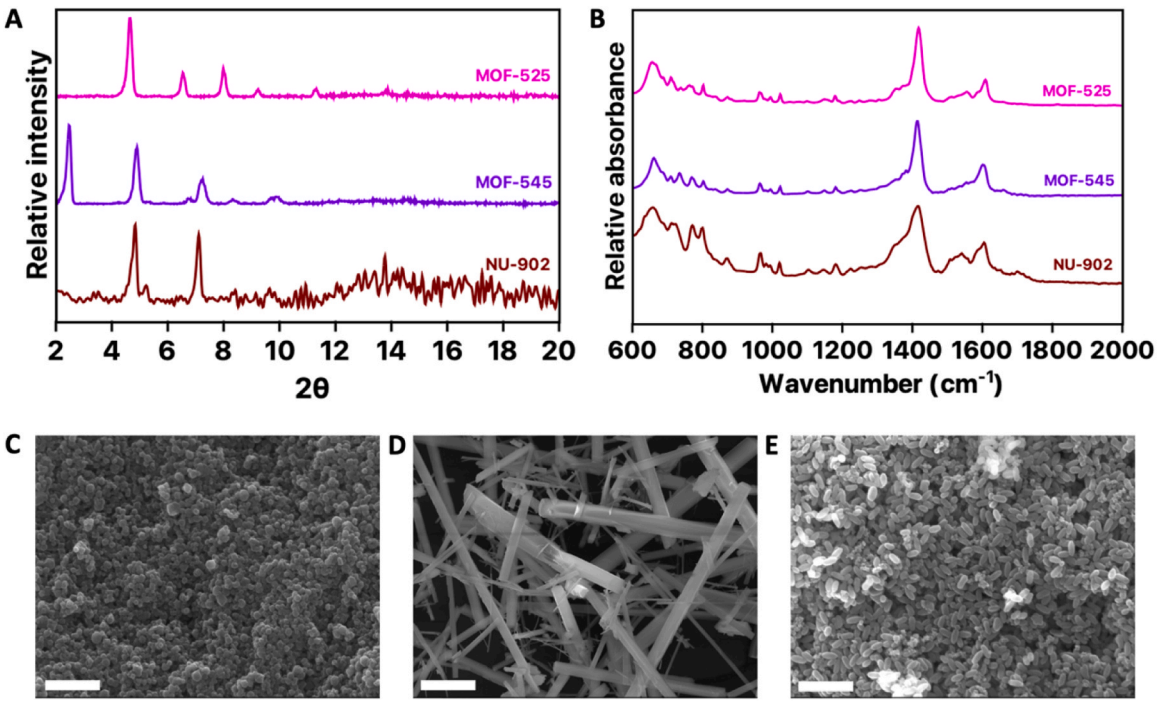


**Fig. 3.** The PXRD patterns (A) and FTIR spectrum (B) of the MOFs used in this study and SEM micrographs of MOF-525 (C), MOF-545 (D) and NU-902 (E). The scalebars for the SEM micrographs are 2 μm, 20 μm and 2 μm for figure C, D and E, respectively.

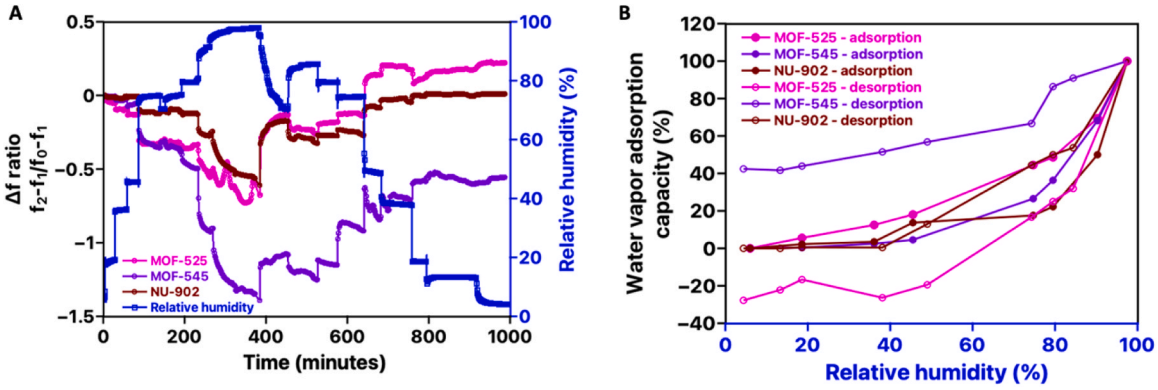


**Fig. 4.** The response of the MOF-525, MOF-545 and NU-902 QCM sensors during extended experiment time (A) and the percentage of water vapor adsorption capacity of the sensors at different relative humidity level (B).

harmonious oscillation of the MOF QCM sensor, resulting in a negative QCM frequency trend instead a positive frequency shift.

During this experiment, the relative humidity was then set between 6 % until 98 % by exposing the samples in the surrounding atmosphere of different salt solutions. From this result, it can be firstly seen that almost negligible water vapor uptake at low relative humidity level (below around 30 %) is observed for all the MOF used in this study. As has been previously stated, the negligible uptake for all the MOFs might be associated with the hydrophobicity of the porphyrin ligand and thus requiring higher partial pressure for the water vapor adsorption to take place [40,42]. Once the relative humidity level goes above around 40 %, the water vapor adsorption starts to take place and the adsorption process continues with the increasing level of the relative humidity. At the highest relative humidity level, it can be observed that MOF-545 shows the highest water vapor uptake followed by MOF-525 and NU-902, respectively. It should also be noted that, as can be also seen from the Fig. 4(A), the highest and lowest water vapor uptake owned by MOF-545 and NU-902, respectively, is actually the material property of the corresponding MOF and is not caused by the difference of the MOF loading on the QCM since we also made sure that similar amount of materials were coated on the QCM sensor. As can also be seen in the Fig. 4(A), the *y* axis is the normalized uptake of the QCM frequency change that has taken into account the difference of the MOF loading on the QCM.

However, despite the fact that MOF-545 shows the highest water vapor uptake, it can also be observed that during the desorption process, the MOF-545 QCM sensor cannot return to its initial state, even after letting the system to equilibrate for around 200 minutes in the last desorption stage. This contrasts with the trend observed in the NU-902 QCM sensor, which can immediately return to its initial state after the desorption process finishes. This is then better depicted in the Fig. 4(B) showing the water vapor uptake value of all the samples at different relative humidity levels during the adsorption and desorption stages, as represented by the change of the QCM frequency. As can be seen in the result, the MOF-545 exhibits a hysteresis since the adsorption-desorption curve does not form a close loop, as observed in the case of

NU-902.

This phenomenon might be attributed firstly to the strong interaction established between the adsorbed water vapor molecules and the MOF-545 framework. Since the MOF-545 exhibits the highest water vapor uptake in comparison to the other samples, it could also mean that its framework has the highest affinity towards water vapor. The second possibility might be caused by the water vapor condensation occurring inside the MOF-545 framework. In this case, the accumulation of water vapor molecules in a certain area of the MOF-545 might lead to the condensation in certain particular regions. Consequently, once adsorbed inside the framework, some of the water vapor molecules may not be reversibly desorbed without the assistance of external driving force, such as heat treatment either because they are too strongly attached to the framework or have condensed. Taking into account that MOF-545 has two distinct pore architecture with diameter around 1 nm and 3.6 nm [43], we could then assume that the water vapor condensation might occur inside the pore structure with diameter around 1 nm since the water vapor capillary condensation might occur more easily in this region rather than in the pore structure with diameter around 3.6 nm.

From the plot shown in the Fig. 4 and the Figure S2 and S3 in the Supplementary Information, it is also evident that there is a difference regarding the sensitivity among all the samples investigated in this study. In the case of NU-902 QCM sensor, we have observed that the QCM frequency barely shifts below 40 % relative humidity. This contrasts with both the MOF-525 and MOF-545 QCM sensors, which already exhibit a change in the QCM frequency when the relative humidity is around 36 %. Specifically, the frequency shift of the MOF-525 and MOF-545 QCM sensor is found to be approximately −48 Hz and −19 Hz, respectively. However, a more pronounced increase in the QCM frequency shift can be observed at around 70 % relative humidity. In this condition, the QCM frequency shift for MOF-525, MOF-545 and NU-902 is found to be approximately −164 Hz, −195 Hz and −48, respectively. As the relative humidity further increases, the QCM frequency shift for all the samples continues to decrease indicating that the saturation point has not been reached for all the samples. At maximum relative humidity, namely 100 %, the QCM frequency shift for MOF-525, MOF-545 and NU-902 is found to be approximately −367 Hz, −720 Hz and −268 Hz respectively.

From this observation, it can be inferred that all the MOF QCM samples used in this study might be suitable for application in the range of relative humidity between 40 % and 70 %. Controlling relative humidity within this range is crucial, as it corresponds to the relative humidity level where human beings feel comfortable [1,2]. Furthermore, since our MOF QCM sensors remain responsive when the relative humidity exceeds 70 %, they could serve as an early warning sign when the relative humidity in an indoor environment surpasses the comfort zone for humans. This contrasts with another MOF-based QCM sensor built from MIL-101(Cr), for example, since in the case of this particular sensor, the saturation point has already been reached at 55 % relative humidity [44]. In that case, when the relative humidity exceeds 55 %, the sensor ceases to response as the change in the QCM frequency shift is no longer observed due to saturation. Additionally, all the MOF QCM sensors in this study remain responsive even when the relative humidity falls below 40 %, as indicated by their change in the QCM frequency shift.

### 3.2. Periodic cycling of sensing

Considering the applicability of our MOF QCM sensors within the range of 40 % and 70 % relative humidity, we performed periodic cycling of the QCM sensors between approximately 35–45 % and 70 % relative humidity to investigate the repeatability of the sensor response, as shown in the Fig. 5. Initially, all the QCM sensors exhibited good response repeatability in the first three cycles. During the first cycle, when the relative humidity was set to 70 %, all the QCM sensors reached the saturation point in less than 10 minutes. Subsequently, when the relative humidity was switched back to around 45 %, almost all the response of the QCM sensors returned to their initial levels.

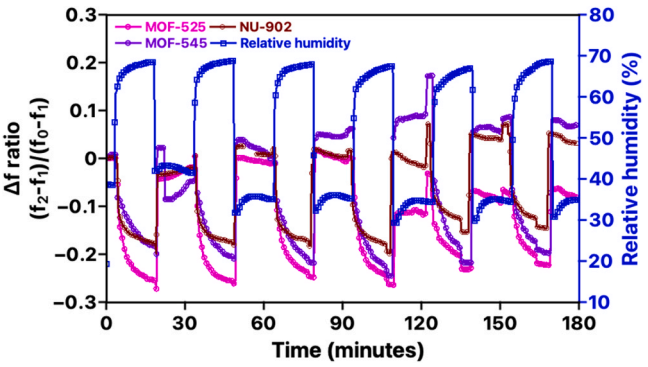


**Fig. 5.** The periodic cycling experiment of MOF-525, MOF-545 and NU-902 QCM sensors between relative humidity of 40 % and 70 %.

However, a deviation in QCM response was observed for MOF-545. In this case, as can be seen from the result, the initial state of the MOF-545 sensor could not be reached as the QCM frequency of this particular sensor remained slightly lower than the initial state. As will be further discussed, such a deviation occurred not because the MOF-545 is unable to completely desorb the water vapor molecule from its framework but because of its high sensitivity towards a slight change in the relative humidity within this range. During the first cycle, the relative humidity was brought back to be approximately 40–45 %, slightly higher than the initial value, namely 35 %. As a result, some of the water vapor adsorbed on MOF-545 cannot be completely released from its framework. However, as can be seen in the second and third cycle, the MOF-545 QCM sensor was able to return to its initial state when the relative humidity was brought back to around 35 %.

The ability of the MOF-545 to completely gain its initial state during this periodic study differs from the trend observed during the extended adsorption-desorption experiment as explained in the Section 3.1. During the extended experiment, the MOF-545 QCM sensor could not return to its initial state after the desorption process finished. However, in the current case, the MOF-545 QCM sensor shows a good repeatability until the last cycle. This discrepancy might be associated with the absence of the irreversible adsorption sites within the MOF-545 framework. Since some of the water vapor molecules have been irreversibly adsorbed during the extended experiment, these adsorption sites were no longer accessible to the incoming water vapor molecules during the periodic cycling experiment. Consequently, all the water vapor molecules adsorbed in the MOF-545 framework could only occupy the reversible adsorption sites and could be reversibly released without requiring external assistance. This is also supported by the absolute value of the frequency change of MOF-545, where the QCM frequency shift at 70 % relative humidity is approximately −100 Hz, which is lower than the value obtained during the extended experiment in the Section 3.1 where it reaches around −195 Hz. This strongly indicates that some of the irreversible adsorption sites of MOF-545 were fully occupied, leaving behind only reversible adsorption sites.

After the first three cycles, both MOF-545 and NU-902 QCM sensors exhibited good response repeatability, as they could return to their initial conditions once the relative humidity was switched back to 35 %. However, a different condition was observed for the MOF-525 QCM sensor. Starting from the fourth cycle, the initial state of the MOF-525 could no longer be reached when the relative humidity was brought back to around 35 %. The QCM response frequency of the MOF-525 QCM sensor at this condition remained around −50 Hz, lasting until the end of the measurement. Unlike in the previous case observed in MOF-545 during the initial period of the periodic cycling experiment, this condition might indicate the irreversible adsorption of the water vapor within the MOF-525 structure. This is supported by closer

observation of the MOF-525 QCM sensor trend when the relative humidity in the system was increased to 70 %. As can be seen, the frequency of the MOF-525 QCM sensor tended to be higher during the first cycling periods. In the first cycle, it exhibited higher adsorption than MOF-545 QCM sensor. However, starting from the third cycle, the QCM response of the MOF-525 started to approach the MOF-545 at 70 % relative humidity. By the fourth cycle, both MOF-525 and MOF-545 QCM response were almost equal. This indicates that the MOF-525 QCM was not able to desorb all the adsorbed water vapor at the given timeframe of the periodic cycling (20 minutes). Consequently, there might have been an accumulation of water vapor within the MOF-525 framework, resulting in the water vapor condensation that could not be effectively desorbed during this cycling experiment simply by changing the relative humidity of the surrounding environment. Therefore, this suggests that the MOF-525 might require more time to completely desorb the water vapor from its framework or, when the timeframe is very limited, it might require the additional assistance (e.g., thermal treatment) to completely desorb all the adsorbed water vapor from its framework.

This phenomenon could then be associated with the pore architecture difference between MOF-525 and MOF-545. The pore size of MOF-525 is estimated to be around 2 nm [43]. Meanwhile, as has been previously stated, MOF-545 has two distinct pores with diameter around 1 nm and 3.6 nm [43]. As has been previously discussed in the extended experiment (Section 3.1), an irreversible adsorption phenomenon was observed in MOF-545 and this might happen in the MOF-545's pores with diameter around 1 nm. Therefore, during the periodic cycling experiment, the adsorption sites of MOF-545 is left within its mesoporous structure with diameter around 3.6 nm. In contrast, the adsorption sites of MOF-525 is served within the pore structure with diameter around 2 nm since it could be assumed that MOF-525 was completely empty at the beginning of the periodic cycling experiment since we did not observe irreversibility during the first extended experiment as in the case of MOF-545. Since the pore diameter of MOF-525 is smaller than MOF-545, as a consequence, water vapor condensation could occur more easily in MOF-525 rather than MOF-545 and it might also be more difficult for the water vapor molecule to be completely desorbed from the MOF-525 framework than MOF-545. Therefore, if no sufficient time is given to the MOF-525 for complete desorption, the water vapor starts to condense and thus resulting in the irreversibility as observed in this periodic cycling experiment. Meanwhile, with bigger pore diameter, the water vapor molecule might be easier to be completely desorbed from the MOF-545 framework and thus resulting in a better relative humidity sensor performance as indicated by the absence of the irreversibility during this period cycling experiment.

Lastly, we analyzed the kinetic response of all the QCM sensors and the results are presented in the Fig. 6. From the adsorption kinetic analysis, we fit the data by Langmuir adsorption isotherm model [45–47]. Based on this model, the change of QCM frequency can be correlated with the adsorption-desorption rate as shown in the Eq. (1)

$$\frac{d\Delta f}{dt} = (\Delta f_{\max} - \Delta f)k_a C - k_d \Delta f \tag{1}$$

where $\Delta f_{max}$ is the maximum frequency change, $C$ is the concentration of the adsorbed water vapor molecules, $k_a$ and $k_d$ corresponds to the adsorption and desorption rate, respectively. The solution for the Eq. (1) yields the Eq. (2) as given below

$$\Delta f(t) = \Delta f_{\max} K' \left(1 - e^{-k_{obs} t}\right) = b1\left(1 - e^{-b2t}\right) \tag{2}$$

where $K'$ is the association constant and $k_{obs}$ is the inverse of the relaxation time. The adsorption rate is then fitted based on this equation where $b1$ is the product of $\Delta fmax$ and K' while $k_{obs}$ is represented as $b2$.

From the above equation, it is evident that the NU-902 QCM sensor has the highest $b2$ value ($3.3 \times 10^{-2}$) and almost one order of magnitude higher than MOF-525 ($7.6 \times 10^{-3}$) and MOF-545 ($5.1 \times 10^{-3}$) QCM sensor. This indicates that the adsorption response of the NU-902 QCM sensor could be considered as the fastest among the samples used in this study. Despite this advantage, this could not warrant the use of NU-902 as a reliable sensitive material for relative humidity sensor in an indoor setting because of its lack of sensitivity at low relative humidity level below 40 %.

Meanwhile, for the desorption kinetic, we fit the data using the one-phase exponential decay equation as shown in the Eq. (3).

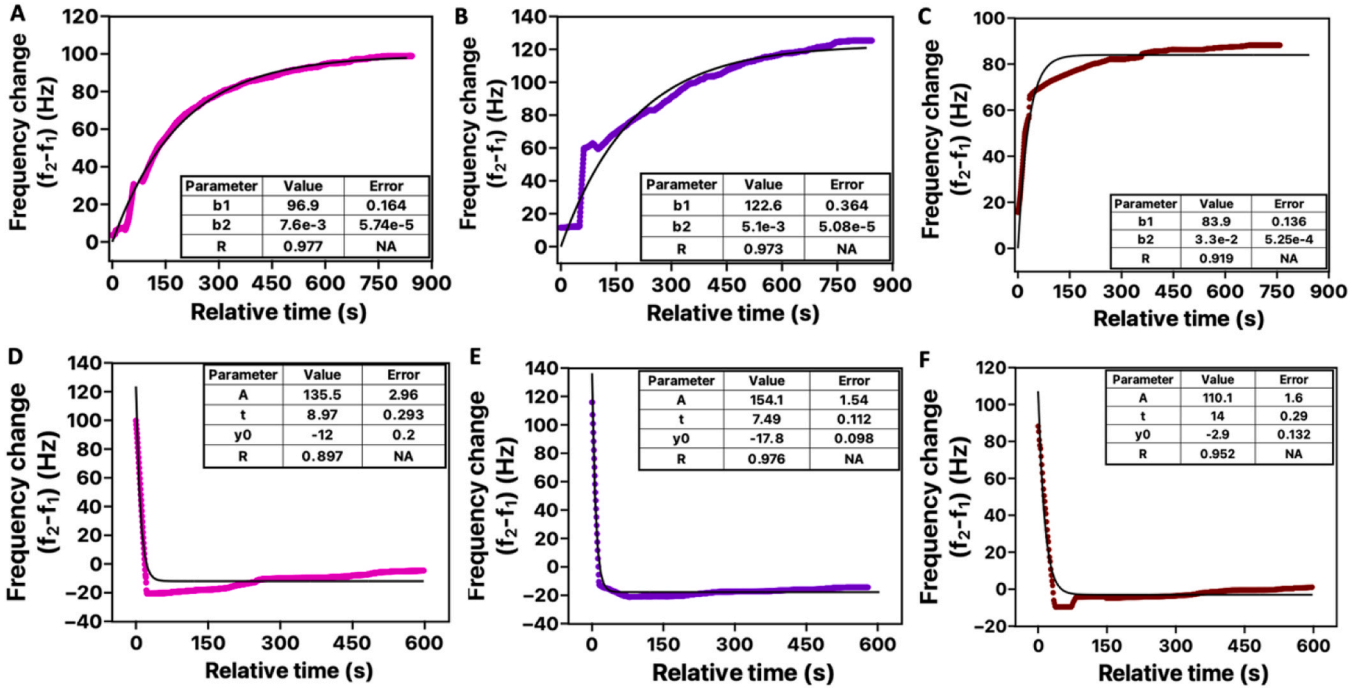


**Fig. 6.** The analysis of the water vapor adsorption and desorption kinetic of MOF-525 (A and D), MOF-545 (B and E) and NU-902 (C and F).

$$y = y0 + A \times \exp\left(-\frac{x}{t}\right) \quad (3)$$

where *y0* is the offset, *A* is the amplitude and *t* is the time constant. In contrast to the water vapor adsorption kinetics, the water vapor desorption trend for all of the samples shows a similar trend. It is also corroborated from the time constant *t* for all the samples which is not very different from each other, namely in the range of 7.5–14 s. This suggests that all the samples can rapidly desorb the adsorbed water vapor from their framework at relatively the same rate. It is important to note that the desorption here might only occur for the water vapor molecules that can be desorbed within the given timeframe. As discussed previously during the periodic cycling experiment, in the case of MOF-525 QCM sensor, some of the water vapor molecules might not be desorbed from the MOF-525 framework due to the relatively short desorption time or the lack of the sufficient desorption driving force, leading to accumulation.

Based on the comprehensive analysis conducted, it could be concluded that the MOF-545 QCM sensor demonstrates the best performance for application as a relative humidity sensor applied in the indoor settings. This conclusion is supported by its high sensitivity across the entire relative humidity range of 40–70 %, making it suitable for maintaining optimal indoor relative humidity levels. In contrast, while the NU-902 offers good repeatability, it lacks sensitivity at low relative humidity levels. Additionally, in comparison to the MOF-545, the MOF-525 requires more time for complete desorption of water vapor from the framework which might lead to the adsorption irreversibility and thus deterioration of the sensor performance once the water vapor starts to condense inside the framework. However, it is important to note that the successful deployment of MOF-545 as the relative humidity sensor requires preliminary treatment to address its irreversible adsorption sites. Failure to address this issue may compromise the sensor's repeatability. Therefore, before practical implementation, attention must be given to filling these irreversible adsorption sites to ensure consistent and reliable sensor operation.

In summary, the MOF-545 QCM sensor emerges as the most promising option for indoor relative humidity sensing applications, offering sensitivity across a wide range of relative humidity levels. However, it is essential to address its inherent limitations to achieve optimal performance in real-world indoor environments.

## 4. Conclusions

In conclusion, in this study, we have systematically investigated the efficacy of three Zr free-base porphyrin MOFs, namely MOF-525, MOF-545 and NU-902, as the QCM-based relative humidity sensors. Through the extended water vapor adsorption-desorption experiments at different relative humidity level, distinct behaviors for each MOF have been observed. MOF-545 exhibited strong water vapor molecule adsorption, preventing it from returning to its initial state post-desorption. Meanwhile, MOF-525 and NU-902 demonstrated almost a closed loop of water vapor adsorption-desorption. All the MOF QCM sensors showed responsiveness to water vapor molecules at varying relative humidity levels, particularly above 40 % and up to 100 %. This sensitivity makes them highly suitable for controlling the relative humidity levels in indoor environments, where maintaining relative humidity between 40 % and 70 % is crucial for human comfort.

To further confirm this possibility and to measure the repeatability of our sensors, we carried out the periodic cycling study using all the three sensors by exposing them to relative humidity between 40 % and 70 %. Interestingly, during this experiment, MOF-545 could maintain the measurement repeatability and also show high sensitivity. This is in contrast to its behavior during the extended experiment phase where it showed irreversible adsorption-desorption behavior. This then puts MOF-545 at a slight edge in comparison to the other MOFs used in this study. In the case of MOF-525, an irreversible behavior was observed and might indicate the requirement of longer time or external assistance to completely desorb the water vapor from its framework. Meanwhile, the NU-902 has exhibited the lack of sensitivity at low relative humidity levels. However, it is essential to note that preliminary treatment of MOF-545 may be necessary to address its irreversible adsorption sites to ensure the measurement repeatability before its deployment as a relative humidity sensor for various indoor settings. In summary, it can be concluded that MOF-545 stands out as the optimal choice for the indoor relative humidity sensing applications due to its sensitivity and repeatability, provided appropriate measures are taken to address its inherent limitations.

## CRediT authorship contribution statement

**Nicholaus Prasetya:** Writing – review & editing, Writing – original draft, Visualization, Validation, Supervision, Software, Resources, Project administration, Methodology, Investigation, Funding acquisition, Formal analysis, Data curation, Conceptualization. **Salih Okur:** Writing – review & editing, Validation, Supervision, Software, Resources, Methodology, Investigation, Formal analysis, Data curation, Conceptualization.

## Declaration of Competing Interest

The authors declare that they have no known competing financial interests or personal relationships that could have appeared to influence the work reported in this paper.

## Data availability

Data will be made available on request.

## Acknowledgements

N. P acknowledges the funding from the Alexander von Humboldt Postdoctoral Fellowship (Ref 3.3 – GBR – 1219268 – HFST-P). S.O acknowledges the support from Helmholtz Funding Program Oriented Research IV, Key Technology Program 43 Program Material Systems Engineering (MSE). The authors also acknowledge the assistance from Dr. Chatrawee Direksilp for materials characterization.

## Appendix A. Supporting information

Supplementary data associated with this article can be found in the online version at doi:10.1016/j.sna.2024.115713.

## References

[1] Z. Rao, S. Wang, Z. Zhang, Energy saving latent heat storage and environmental friendly humidity-controlled materials for indoor climate, Renew. Sustain. Energy Rev. 16 (2012) 3136–3145.
[2] O. Watanabe, E.H. Ishida, H. Maeda, Development of an autonomous humidity controlling building material by using mesopores, Trans. Mater. Res. Soc. Jpn. 33 (2008) 489–492.
[3] L. Reinikainen, J. Jaakkola, Significance of humidity and temperature on skin and upper airway symptoms, Indoor Air 13 (2003).
[4] G. Blomquist, F. Gyntelberg, B. Järvholm, P. Malmberg, L. Nordvall, A. Nielsen, G. Pershagen, J. Sundell, Dampness in buildings and health: nordic interdisciplinary review of the scientific evidence on associations between exposure to "Dampness" in buildings and health effects (NORDDAMP), Indoor Air 11 (2001) 72–86.
[5] E. Owji, H. Mokhtari, F. Ostovari, B. Darazereshki, N. Shakiba, 2D materials coated on etched optical fibers as humidity sensor, Sci. Rep. 11 (2021) 1771.
[6] Y. Zhang, B. Fu, K. Liu, Y. Zhang, X. Li, S. Wen, Y. Chen, S. Ruan, Humidity sensing properties of FeCl3-NH2-MIL-125 (Ti) composites, Sens. Actuators B: Chem. 201 (2014) 281–285.
[7] S. Sikarwar, B. Yadav, Opto-electronic humidity sensor: a review, Sens. Actuators A: Phys. 233 (2015) 54–70.
[8] N. Yamazoe, Y. Shimizu, Humidity sensors: principles and applications, Sens. Actuators 10 (1986) 379–398, https://doi.org/10.1016/0250-6874(86)80055-5.

[9] F. Fauzi, A. Rianjanu, I. Santoso, K. Triyana, Gas and humidity sensing with quartz crystal microbalance (QCM) coated with graphene-based materials–A mini review, Sens. Actuators A: Phys. 330 (2021) 112837.
[10] Y. Yao, X. Chen, X. Li, X. Chen, N. Li, Investigation of the stability of QCM humidity sensor using graphene oxide as sensing films, Sens. Actuators B: Chem. 191 (2014) 779–783.
[11] N. Gao, H.-Y. Li, W. Zhang, Y. Zhang, Y. Zeng, H. Zhixiang, J. Liu, J. Jiang, L. Miao, F. Yi, QCM-based humidity sensor and sensing properties employing colloidal SnO2 nanowires, Sens. Actuators B: Chem. 293 (2019) 129–135.
[12] K. Ocakoglu, S. Okur, Humidity sensing properties of novel ruthenium polypyridyl complex, Sens. Actuators B: Chem. 151 (2010) 223–228.
[13] N.A. Tehrani, I.C. Esfahani, H. Sun, Simultaneous humidity and temperature measurement with micropillar enhanced QCM sensors, Sens. Actuators A: Phys. 366 (2024) 115039, https://doi.org/10.1016/j.sna.2024.115039.
[14] D. Zhang, D. Wang, P. Li, X. Zhou, X. Zong, G. Dong, Facile fabrication of high-performance QCM humidity sensor based on layer-by-layer self-assembled polyaniline/graphene oxide nanocomposite film, Sens. Actuators B: Chem. 255 (2018) 1869–1877.
[15] Z. Yuan, H. Tai, Z. Ye, C. Liu, G. Xie, X. Du, Y. Jiang, Novel highly sensitive QCM humidity sensor with low hysteresis based on graphene oxide (GO)/poly (ethyleneimine) layered film, Sens. Actuators B: Chem. 234 (2016) 145–154.
[16] P. Qi, T. Zhang, J. Shao, B. Yang, T. Fei, R. Wang, A QCM humidity sensor constructed by graphene quantum dots and chitosan composites, Sens. Actuators A: Phys. 287 (2019) 93–101, https://doi.org/10.1016/j.sna.2019.01.009.
[17] X. Ding, X. Chen, X. Chen, X. Zhao, N. Li, A QCM humidity sensor based on fullerene/graphene oxide nanocomposites with high quality factor, Sens. Actuators B: Chem. 266 (2018) 534–542.
[18] N. Horzum, D. Taşçıoglu, S. Okur, M.M. Demir, Humidity sensing properties of ZnO-based fibers by electrospinning, Talanta 85 (2011) 1105–1111.
[19] L. Pilz, C. Natzeck, J. Wohlgemuth, N. Scheuermann, S. Spiegel, S. Oßwald, A. Knebel, S. Braese, C. Wöll, M. Tsotsalas, Utilizing machine learning to optimize metal-organic framework-derived polymer membranes for gas separation, J. Mater. Chem. A (2023).
[20] X. Zhang, J. Qiao, Y. Jiang, F. Wang, X. Tian, Z. Wang, L. Wu, W. Liu, J. Liu, Carbon-based MOF derivatives: emerging efficient electromagnetic wave absorption agents, Nano-Micro Lett. 13 (2021) 1–31.
[21] Q. Qian, P.A. Asinger, M.J. Lee, G. Han, K. Mizrahi Rodriguez, S. Lin, F. M. Benedetti, A.X. Wu, W.S. Chi, Z.P. Smith, MOF-based membranes for gas separations, Chem. Rev. 120 (2020) 8161–8266.
[22] M.F. Ghazvini, M. Vahedi, S.N. Nobar, F. Sabouri, Investigation of the MOF adsorbents and the gas adsorptive separation mechanisms, J. Environ. Chem. Eng. 9 (2021) 104790.
[23] N. Prasetya, I.G. Wenten, M. Franzreb, C. Wöll, Metal-organic frameworks for the adsorptive removal of pharmaceutically active compounds (PhACs): comparison to activated carbon, Coord. Chem. Rev. 475 (2023) 214877.
[24] M. Mon, R. Bruno, J. Ferrando-Soria, D. Armentano, E. Pardo, Metal–organic framework technologies for water remediation: towards a sustainable ecosystem, J. Mater. Chem. A 6 (2018) 4912–4947.
[25] L.E. Kreno, K. Leong, O.K. Farha, M. Allendorf, R.P. Van Duyne, J.T. Hupp, Metal–organic framework materials as chemical sensors, Chem. Rev. 112 (2012) 1105–1125.
[26] W. Cheng, X. Tang, Y. Zhang, D. Wu, W. Yang, Applications of metal-organic framework (MOF)-based sensors for food safety: enhancing mechanisms and recent advances, Trends Food Sci. Technol. 112 (2021) 268–282.
[27] L. Wang, Metal-organic frameworks for QCM-based gas sensors: a review, Sens. Actuators A: Phys. 307 (2020) 111984, https://doi.org/10.1016/j.sna.2020.111984.
[28] N. Prasetya, C. Wöll, Removal of diclofenac by adsorption process studied in free-base porphyrin Zr-metal organic frameworks (Zr-MOFs), RSC Adv. 13 (2023) 22998–23009, https://doi.org/10.1039/D3RA03527A.
[29] K. Yu, I. Ahmed, D.-I. Won, W.I. Lee, W.-S. Ahn, Highly efficient adsorptive removal of sulfamethoxazole from aqueous solutions by porphyrinic MOF-525 and MOF-545, Chemosphere 250 (2020) 126133.
[30] B. Chen, Y. Li, M. Li, M. Cui, W. Xu, L. Li, Y. Sun, M. Wang, Y. Zhang, K. Chen, Rapid adsorption of tetracycline in aqueous solution by using MOF-525/graphene oxide composite, Microporous Mesoporous Mater. 328 (2021) 111457.
[31] W. Morris, B. Volosskiy, S. Demir, F. Gándara, P.L. McGrier, H. Furukawa, D. Cascio, J.F. Stoddart, O.M. Yaghi, Synthesis, structure, and metalation of two new highly porous zirconium metal–organic frameworks, Inorg. Chem. 51 (2012) 6443–6445, https://doi.org/10.1021/ic300825s.
[32] T. Huang, C. Kung, Y. Liao, S. Kao, M. Cheng, T. Chang, J. Henzie, H.R. Alamri, Z. A. Alothman, Y. Yamauchi, Enhanced charge collection in MOF-525–PEDOT nanotube composites enable highly sensitive biosensing, Adv. Sci. 4 (2017) 1700261.
[33] G.-Y. Zhang, Y.-H. Zhuang, D. Shan, G.-F. Su, S. Cosnier, X.-J. Zhang, Zirconium-based porphyrinic metal–organic framework (PCN-222): enhanced photoelectrochemical response and its application for label-free phosphoprotein detection, Anal. Chem. 88 (2016) 11207–11212.
[34] Y.-C. Wang, Y.-C. Chen, W.-S. Chuang, J.-H. Li, Y.-S. Wang, C.-H. Chuang, C.-Y. Chen, C.-W. Kung, Pore-confined silver nanoparticles in a porphyrinic metal–organic framework for electrochemical nitrite detection, ACS Appl. Nano Mater. 3 (2020) 9440–9448.
[35] S. Pal, Y.-Z. Su, Y.-W. Chen, C.-H. Yu, C.-W. Kung, S.-S. Yu, 3D printing of metal–organic framework-Based ionogels: wearable sensors with colorimetric and mechanical responses, ACS Appl. Mater. Interfaces 14 (2022) 28247–28257.
[36] B.J. Deibert, J. Li, A distinct reversible colorimetric and fluorescent low pH response on a water-stable zirconium–porphyrin metal–organic framework, Chem. Commun. 50 (2014) 9636–9639.
[37] K.T. Smith, C.A. Ramsperger, K.E. Hunter, T.J. Zuehlsdorff, K.C. Stylianou, Colorimetric detection of acidic pesticides in water, Chem. Commun. 58 (2022) 953–956.
[38] L. Greenspan, Humidity fixed points of binary saturated aqueous solutions, J. Res. Natl. Bur. Stand. Sect. A, Phys. Chem. 81 (1977) 89.
[39] H. Furukawa, F. Gándara, Y.-B. Zhang, J. Jiang, W.L. Queen, M.R. Hudson, O. M. Yaghi, Water adsorption in porous metal–organic frameworks and related materials, J. Am. Chem. Soc. 136 (2014) 4369–4381.
[40] T. Liu, L. Jing, L. Cui, Q. Liu, X. Zhang, Facile one-pot synthesis of a porphyrin-based hydrophilic porous organic polymer and application as recyclable absorbent for selective separation of methylene blue, Chemosphere 212 (2018) 1038–1046.
[41] N. Prasetya, S. Okur, MOF-composite sensors to eliminate the QCM positive frequency shift, Sens. Actuators B: Chem. (2023) 134507, https://doi.org/10.1016/j.snb.2023.134507.
[42] Marcin. Ptaszek, Chapter Three - Rational Design of Fluorophores for In Vivo Applications, in: M.C. Morris (Ed.), Progress in Molecular Biology and Translational Science, Academic Press, 2013, pp. 59–108, https://doi.org/10.1016/B978-0-12-386932-6.00003-X.
[43] Y. Liu, L. Chen, X. Zhao, X. Yan, Effect of topology on photodynamic sterilization of porphyrinic metal-organic frameworks, Chem. –A Eur. J. 27 (2021) 10151–10159.
[44] P.P. Conti, P. Iacomi, M. Nicolas, G. Maurin, S, Devautour-vinot, MIL-101 (Cr)@ QCM and MIL-101 (Cr)@ IDE as sorbent-based humidity sensors for indoor air monitoring, ACS Appl. Mater. Interfaces 15 (2023) 33675–33681.
[45] R. Demir, S. Okur, M. Seker, M. Zor, Humidity sensing properties of CdS nanoparticles synthesized by chemical bath deposition method, Ind. Eng. Chem. Res. 50 (2011) 5606–5610.
[46] S. Okur, M. Kuş, F. Özel, V. Aybek, M. Yılmaz, Humidity adsorption kinetics of calix [4] arene derivatives measured using QCM technique, Talanta 81 (2010) 248–251.
[47] D. Karpovich, G. Blanchard, Direct measurement of the adsorption kinetics of alkanethiolate self-assembled monolayers on a microcrystalline gold surface, Langmuir 10 (1994) 3315–3322.

**Nicholaus Prasetya, PhD** is currently an Alexander von Humboldt Postdoctoral Research Fellow in the Institute of Functional Interfaces (IFG), Karlsruhe Institute of Technology (KIT), Germany. He completed his PhD at the Department of Chemical Engineering, Imperial College London, United Kingdom (September 2019). His research interests are in the field of the development of metal organic frameworks (MOFs) and their composites for various purposes, including separation and sensing.

**Prof. Salih Okur** received his diploma degree in Physics from the Hacettepe University, Turkey, in 1989 and the Ph.D. degree in Solid State Physics (May 1998) from Illinois Institute of Technology, Chicago, USA. He worked as a Research Assistant (1993–2000), an Assistant Professor (2000–2006), and Associate Professor (2006–20011) in the Department of Physics in the Izmir Institute of Technology, Turkey, before accepting a Full Professor position in the Department of Material Science and Engineering in the University of Katip Celebi. He was the Dean of Engineering Faculty in University of Katip Celebi between 2011 and 2015. His research area comprises nanoparticle materials, surface modification, sensors, QCM based electronic nose. Between 2017 and 2020, he was a Guest Professor in the Light Technology Institute (LTI) of the Karlsruhe Institute of Technology (KIT) and he is now working as a Guest Professor in the Institute of Functional Interfaces (IFG) at Karlsruhe Institute of Technology (KIT).